

# Failure Analysis of the Wire Fixation Bolts of an Ilizarov External Fixator

P. C. Ortega · W. B. Medeiros Jr. · E. Rosa · R. Amorim · G. Cardoso ·  
L. N. Matos · C. R. M. Roesler

Submitted: 9 September 2014 / Accepted: 13 October 2014 / Published online: 7 November 2014  
© ASM International 2014

**Abstract** The Ilizarov method is a treatment used to recover the functionality of the upper and lower limbs of patients who have lost bone tissues due to fractures or/and infections caused by accidents or congenital problems. This technique consists of assembling a device on the patient's limb through which the bone is manipulated gradually. The device consists of external rings connected to each other by threaded rods and fixed to the bone by small diameter steel wires. These wires fasten the bone in an axial cross through a central axis perpendicular to the plane of the bone end and they are tightened to the rings by fixation bolts to provide assembly stability. The proper operation of the device depends mainly on the wire tension, which, in turn, depends on the torque applied to the bolts that hold the wires in place. The failure of these wire fixation bolts may compromise the Ilizarov frame function. In this study, four slotted bolts from a series of slotted bolts fractured during the assembly of Ilizarov fixator in clinical practice were analyzed and the upper limit for tightening these bolts was investigated. The results show that the failures occurred through a combination of mechanical and microstructural factors, including stress concentrators at the upper region of the screw, a high level of microstructural inclusions, and

poor surface finish. The mechanical behavior of the bolts under loads was analyzed using the finite element method with the purpose of correlating it with the failure of the bolts.

**Keywords** Ilizarov external fixator · Wire fixation bolts · Slotted bolt failure

## Introduction

The Ilizarov system is a frame device developed by Grigoriy Ilizarov in Kurgan, Siberia, in 1952. It is used in a specific orthopedic method of external bone fixation. This method relies on the principle of axial compressive loads and micro-movements in the osteogenic zone stimulating biological bone bridging of the fracture gap [1–5]. This explains the success of the Ilizarov system and the reason why it succeeds when other more rigid techniques have failed.

The assembly of the Ilizarov system consists of external rings connected to each other by threaded rods and steel wires and/or pins of small diameter, in addition to elements of fixation connected to the rings (Fig. 1), which, in turn, are connected to other elements such as longitudinal pipes, arches, plates, etc., according to the particularity of each pathology [6]. Transosseous wires, fixed to the steel rings by wire fixation bolts, transfix the bone allowing the stable yet dynamic fixation of the bone fragments [1, 2, 5, 7–10].

The proper functioning of the device depends mainly on the wire tension and its maintenance to limit the micro-movements and the compressive loads at the fracture site [1, 2, 11, 12]. The tension of the wire is maintained by friction force, which varies according to the tightness of the wire fixation bolt. These fixing bolts can be of several types, such

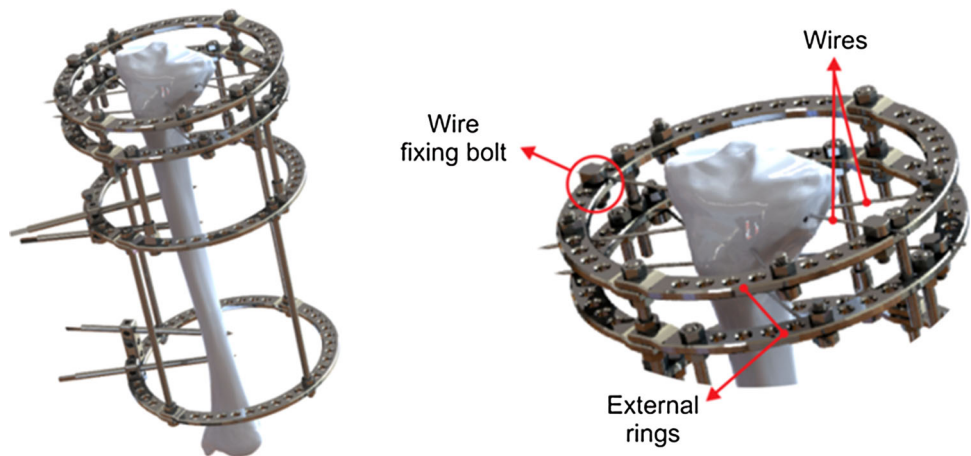
---

P. C. Ortega (✉) · W. B. Medeiros Jr. · C. R. M. Roesler  
Laboratório de Engenharia Biomecânica (LEBm), Hospital  
Universitário, Universidade Federal de Santa Catarina,  
Florianópolis, SC 88040-900, Brazil  
e-mail: patricia.ortega.cubillos@posgrad.ufsc.br

E. Rosa  
GRANTE, Depto. Engenharia Mecânica, Universidade Federal  
de Santa Catarina, Florianópolis, SC 88040-900, Brazil

R. Amorim · G. Cardoso · L. N. Matos  
Hospital Celso Ramos, Secretaria de Saúde de Santa Catarina,  
Florianópolis, SC 88040-900, Brazil

**Fig. 1** Ilizarov device with detailed zoom



as cannulated or slotted, or variations of these two types (for instance, the “Russian” type, which can be seen in [13]).

Ilizarov suggested that the wire tension can be adjusted according to the height and weight of the patient, to provide a scientific approach to frame construction. However, complex interactions between the wire tension and ring diameter, and general configuration of the hardware determine how effectively a frame will work and these have, as yet, not been completely defined mathematically [3, 7, 10, 13, 14].

The pre-tension applied to the wires and supported by the fixation bolts guarantees the device stability. It is very important to control the degree of tightness of the bolts because the friction forces are directly proportional to the normal force. Although the torque is not the best way to control this force, it is the simplest in terms of practical use in the clinical set. Unfortunately, a high degree of bolt shearing during tightening is observed. This raises questions about the bolt design and the quality of the material and its ability to withstand the optimal torque needed to prevent the loss of pre-tension required to achieve a satisfactory treatment.

In this context, the main objective of this study was to analyze the microstructural and mechanical behavior of wire fixing bolts that had previously broken in a clinical set. Fragments of the slotted bolts were characterized in order to evaluate the material and the manufacturing process. Fractographic examination and finite element analysis were carried out to investigate the failure causes and their sequence.

## Materials and Methods

Four broken slotted bolts were analyzed. All bolts had broken during manual tightening performed by the same experienced orthopedic surgeon. The bolts were manufactured using the stainless steel alloy AISI 303 with a



**Fig. 2** Slotted wire fixing bolt of Ilizarov device

nominal size M6 (Fig. 2). For the failure analysis, the specimens were observed both before and after chemical etching using a Nikon Eclipse LV optical microscope and a JEOL JSM-6390LV scanning electron microscope. The inclusions and grain size were measured according to the ASTM E45 and ASTM E112 standards, respectively. The microstructural analysis was carried out on metallographic samples taken from the wire fixation bolts, prepared according to the ASTM E3 standard. The quantitative chemical composition of the fractured fragments of the slotted bolts was determined using a SPECTROMAXx optical emission spectrometer.

Macrofractographic and microfractographic analysis of the fracture surface and its surrounding area was carried out. Observations were made using an Optika stereomicroscope and a JEOL JSM-6390LV scanning electron microscope. These tests were complemented with microhardness measurements carried out on the cross section of the component following the ASTM E384 standard. The roughness of the bolts was measured with a NanoFocus usurf confocal three-dimensional microscope.

In order to acquire a deeper insight into the strain and stress distribution in the wire fixation bolts during loading, the load condition was reproduced virtually and analyzed using Finite Element Analysis (FEA). The mechanical behavior of the bolts under load was correlated with the failure surface characteristics.

## Results and Discussion

### Chemical Composition

The chemical composition of the stainless steel used to manufacture these external bolts differs from that of the material used in bolts for osteosynthesis, which follow the standard ASTM F138.

When the slotted bolt is machined during manufacturing, the standard ASTM F899 for surgical instruments recommends the use of austenitic stainless steel AISI 303, which has a high concentration of sulfur [15].

The results obtained from both fractured and undamaged regions revealed a homogeneous chemical composition close to that of austenitic stainless steel AISI 303.

The data in Table 1 also indicate that the chemical composition of the tested specimens matches the recommended composition of the standard, except that the sulfur

concentration was slightly lower than the minimum specified.

However, the sulfur concentration observed (0.142%) is considerably higher than that of a conventional austenitic stainless steel, which does not exceed 0.040%. This higher concentration of sulfur can lead to an increase in the amount of inclusions, which adversely affects the mechanical strength of the slotted bolts [16].

### Microstructural Analysis

The microstructural analysis of the slotted bolts revealed a homogenous morphology (Fig. 3) along the transverse plane and a highly oriented structure along the longitudinal plane. Based on their chemical composition, the structures were made of a very fine austenite. This alloy has a grain size number of 6 or finer, which was measured in accordance with the ASTM E112 standard. Also slip bands and martensitic ripples were observed, as detailed in Fig. 4, which originate from the manufacturing process and increase the mechanical strength of the material [17]. The original amount of slip bands and martensitic ripples increases due to hardening during the tightening of the bolt, consequently, increasing even further the mechanical strength of the material. This can be seen by comparing the alloy hardness of an intact slotted bolt (236 HB) and that of a fractured bolt (258 HB).

**Table 1** Composition of bolts

Materials	wt. %										
	C	Mn	P	S	Si	Cr	Ni	Mo	N	Cu	Fe
AISI 303	0.15 max	2.00 max	0.2 max	0.15 min	1.00 max	17.00–19.00	8.00–10.00	0.6 max			Balance
Slotted bolt	0.039	1.836	0.038	0.142	0.207	17.369	8.469	0.222	0.035	0.197	

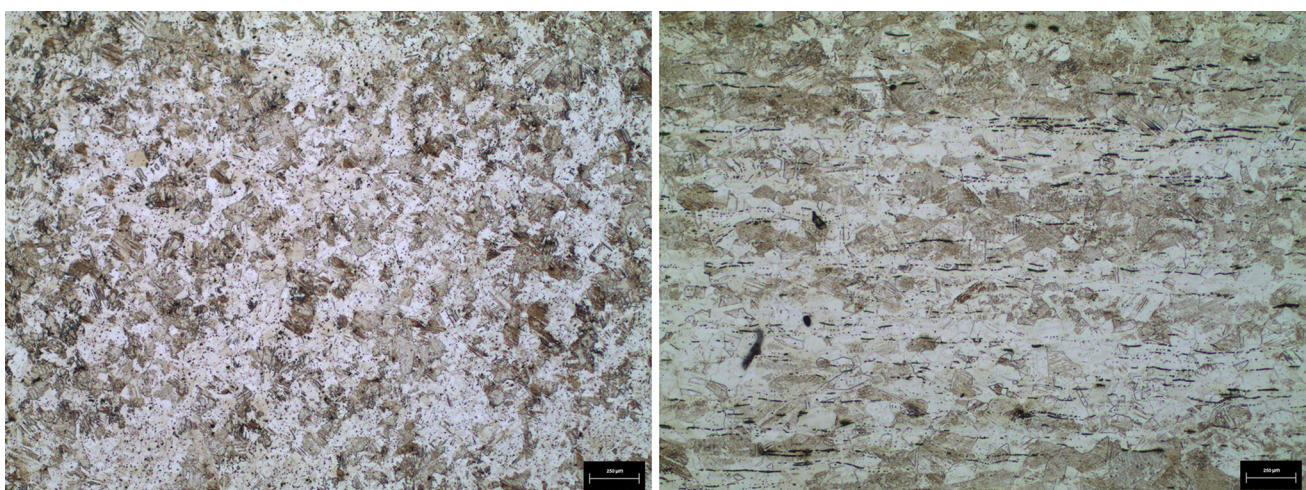


**Fig. 3** Microstructure in transversal and longitudinal planes of fractured bolt ×100

Inclusions in the microstructure were observed as shown in Fig. 4. These inclusions are, in general, comprised manganese sulfide, formed when there is a high concentration of sulfur in the alloy, as shown in Fig. 5, where is possible to observe the micrographic and chemical composition of these inclusions. The severity level of the inclusions in the alloy was found to be 2.0 in the heavy series, according to the ASTM E45 standard. The quantity of inclusions in the slotted bolts is high when compared with biomedical stainless steel, according to the F138 standard, where the maximum severity for the heavy series is 1.5 [18].

Fractographic Analysis

The fracture shown in Fig. 6 is characterized by a spiral texture on the surface which is common in ductile shearing

fractures. This is possible because the slotted bolts have a good shearing ductility, even though they are obtained by hot working [19]. Also inclusions and cracks can be observed on the transversal surface, the latter being formed through the nucleation, growth, and coalescence of microvoids (dimples).

Figure 7 shows that the surface is characterized by a dimpled morphology. The dimples are formed around the inclusions and oriented uniformly in the direction of deformation, as can be observed in the different regions presented in Fig. 6 and extended in Fig. 7. In this case, the failure micromechanism is the dimples and the mechanism is plastic collapse with high shearing strain.

A detail of the beginning of the cracks on the lateral surface in the thread valley next to the head of the slotted bolt is shown in the Fig. 8. The cracks are located on the screw and in the machining scratches. In this case, the machining scratches on the surface of the screw are coarse and act as stress concentrators, contributing to the nucle-

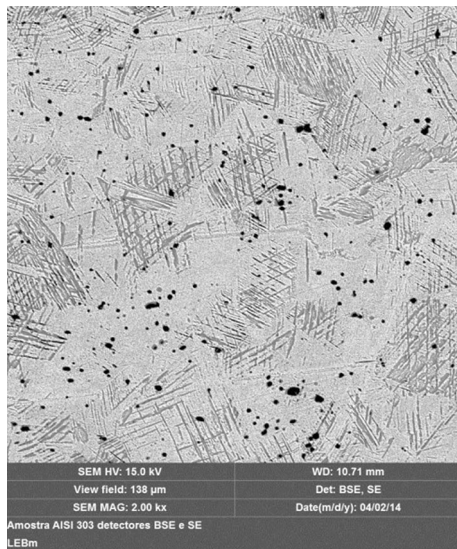


Fig. 4 Fine austenite evidencing inclusions, slip bands, and martensitic ripples ×500

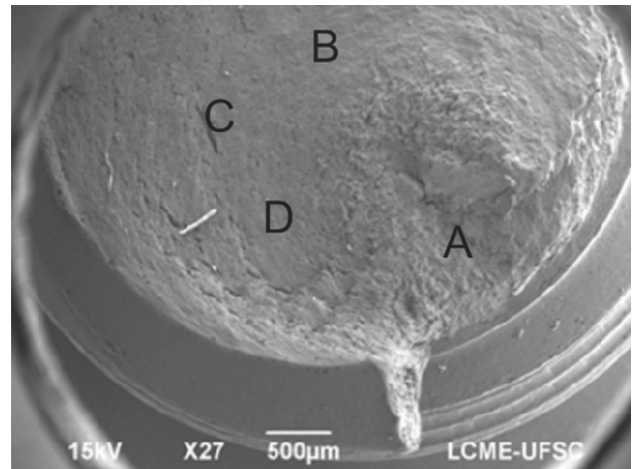


Fig. 6 Fracture surface ×27

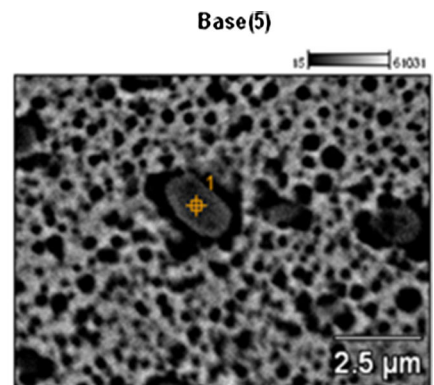
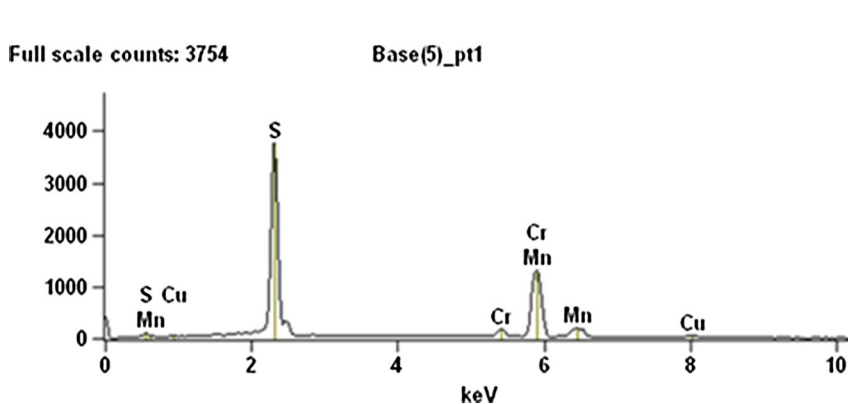
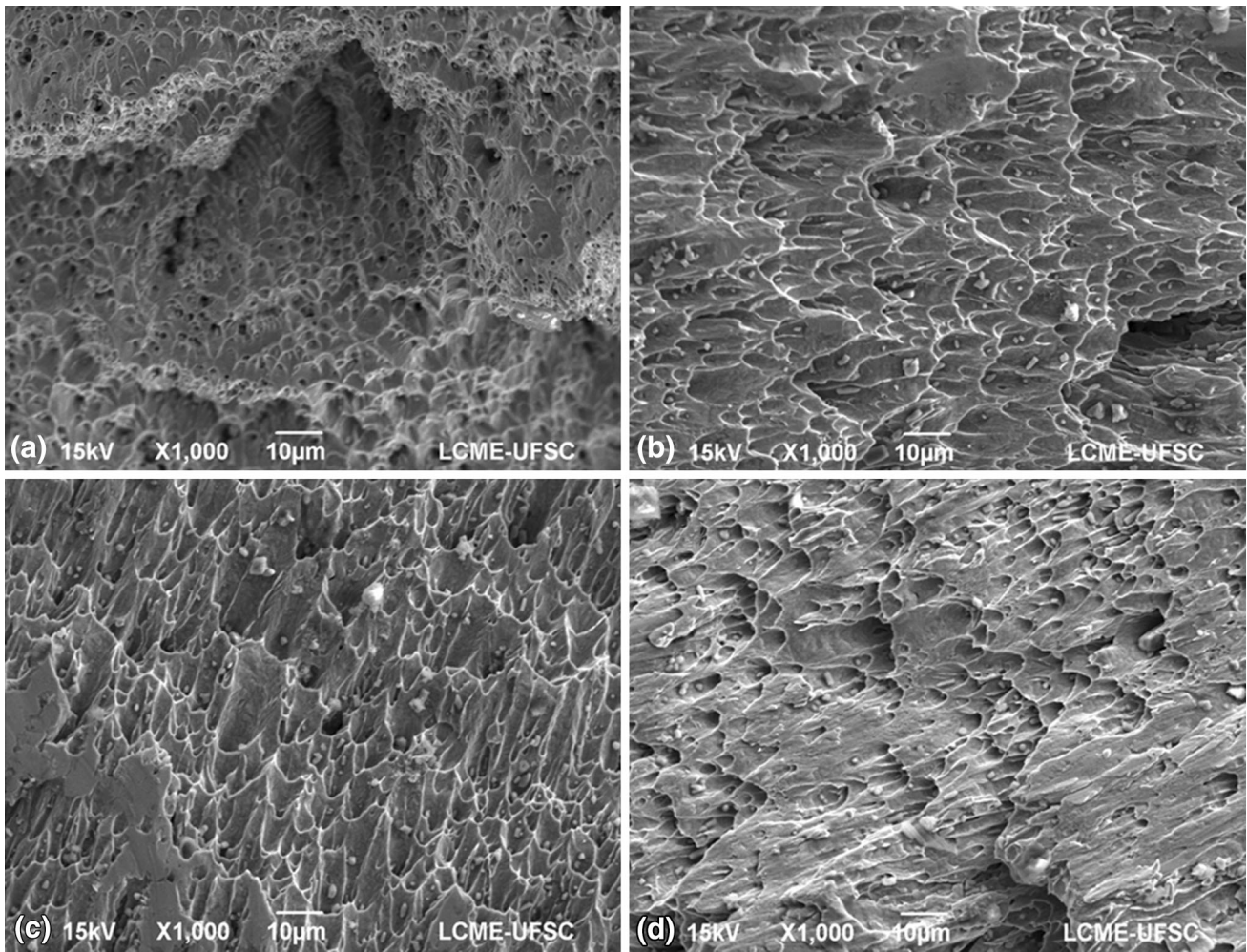
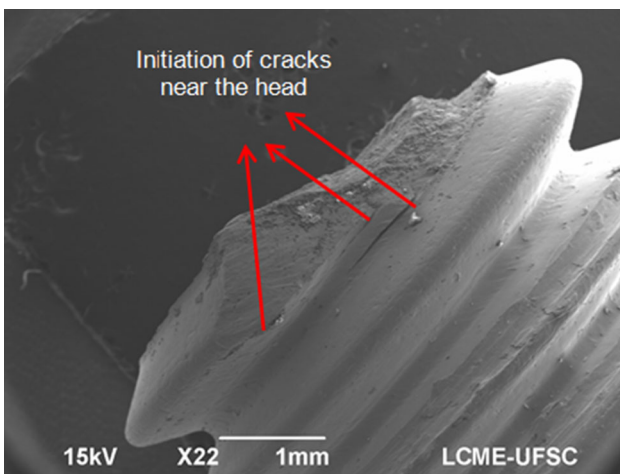


Fig. 5 Inclusions in the austenite matrix



**Fig. 7** Morphology and orientation of the dimples on the fracture surface  $\times 1000$



**Fig. 8** Surface quality of the slotted bolt

ation of the cracks, and multiple cracks are generated in the slotted bolts under torsional load [20]. The roughness was measured and found to be 0.0677 micrometers (*Ra*).

### Mechanical Analysis

The stress distribution and the mechanical properties of the material determine the characteristics of the fracture surface of wire fixation bolts. The tightness of the bolt joints causes deformation and elongation of the bolt. In the elastic regime, the deformation is responsible for producing an effective force that locks the joint. This force is called the preload and the bolt is submitted to tensile stress. According to continuum mechanics, the general stress state of a bolt subjected to axial and torsion loads is shown in Fig. 9.

Besides the tensile stresses, there are also shear stresses in the threads due to the friction between the nut thread and the bolt thread. This shear stress can produce tearing of the screw threads. Since the object of this study is a fractured bolt core, the shear stresses in the screw threads will be neglected.

During the assembly, when a nut is tightened, torsion is transmitted to the bolt. The torque that twists the bolt is

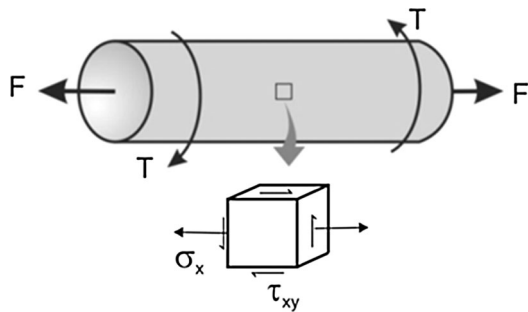


**Fig. 9** Stress state of an element of a cylinder submitted to torsion and axial load

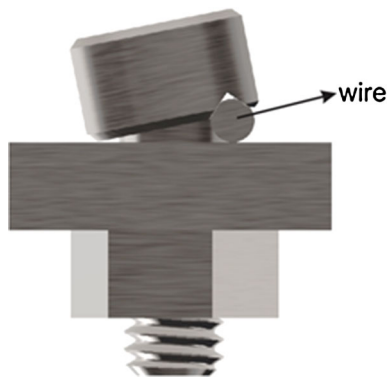


**Fig. 10** Bending of the slotted bolt caused by the wire

dependent on the friction at the bolt–nut interface. If the bolt and nut are well lubricated, a smaller portion of the applied torque is transmitted to the bolt. To include the worst case of friction in the threads, the total torque applied during the tightening can be considered.

Another type of load which can appear is bending, since the nut faces can be not perpendicular to the bolt head. Bending loads can come from two primary sources. The first is direct bending applied to the bolt during the preload phase due to geometric effects and the second is a bending load applied to the structure that must be transmitted through the bolted joint [21]. For the slotted bolts analyzed in this study, the former is responsible for the bending load, since during the preloading, the faces of the bolt head and nut become no longer perpendicular to each other, because the wire is supported by only one side of the screw, although the slot eases this effect (Fig. 10).

The tensile stress in a bolt can be calculated using the diameter,  $d$ , as the diameter where the preload,  $F$ , is applied. A general relationship between the applied torque,  $T$ , and the preload,  $F$ , in the bolt, can be written in terms of the diameter of the bolt,  $d$ , and the factor  $K$ , which is called the nut factor as follows [22]:

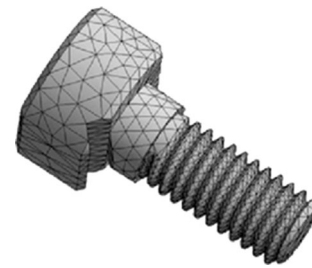


**Fig. 11** Finite elements mesh of the fixation screw

$$T = K \times d \times F \quad (\text{Eq 1})$$

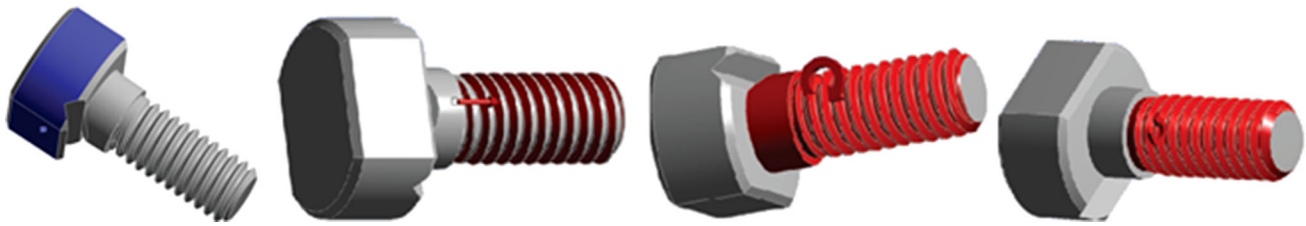
The nut factor can be computed by many methods, but the use of analytical equations is not recommended since, although they aid an understanding of the factors associated with the nut factor, they seem to produce nut factors that are much larger than the experimentally accepted values [21]. An approximation to the value of  $K$  typically used is  $K = 0.2$ . This nut factor is a mean value for general cases, regardless of the type of screw [22].

In order to acquire a deeper insight into the distribution of the strain and stresses occurring in the complex geometry of a bolt, a unitary torque and its respective force (given by Eq (1) for  $K = 0.2$  and  $d = 0.0044$  m) with the momentum caused by the wire were reproduced virtually and analyzed using FEA in a commercial software program (ANSYS Workbench®). To this aim, a mesh of tetrahedral elements was generated for the 3D geometry of the screw, obtained from the CAD software and manual measurements using instruments. The elements used were those of the standard Solid187 and the number of elements was 9970 with 17,017 nodes. The mesh is shown in Fig. 11.

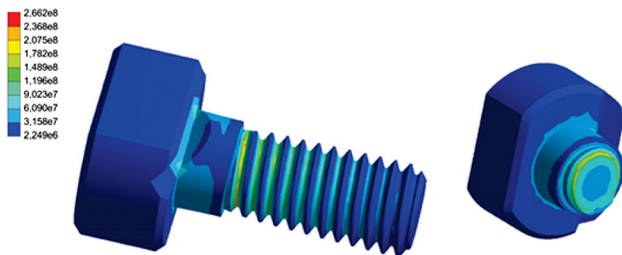
The head geometry was fixed, unitary torque was applied to the threads and the bolt core, an axial load value of 1136.4 N was applied on the upper face of the threads, and a “wire momentum” of 2.272 Nm was applied to threads and core, as shown in Fig. 12. The material properties used in the analysis were density  $7850 \text{ kg m}^{-3}$ , yield strength 250 MPa, Young’s modulus 210 GPa, ultimate tensile strength 460 MPa, and Poisson’s ratio 0.3.

Figure 13 shows the von Mises stresses of the screw for the given load case. The result shows a concentration of stress in the thread valley next to the head of the bolt, which appears at the same site where the fracture origin was observed in the real case specimens. A transversal cut where the maximum stress occurs shows the von Mises stress distribution at bolt core.

The principal stress vectors obtained from the FEA indicate an anticlockwise orientation when a cut parallel to the head face is observed (Fig. 14). The result orientation is



**Fig. 12** Boundary conditions of the model



**Fig. 13** Distribution of the von Mises stress for the loaded fixation screw

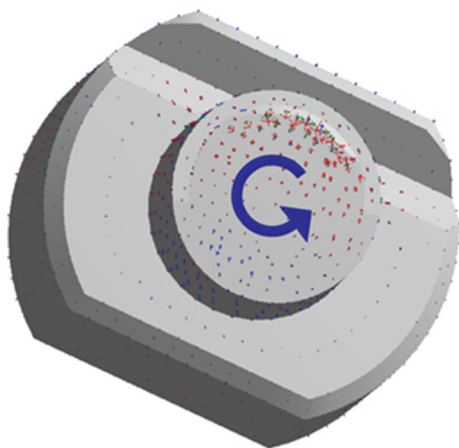


**Fig. 14** Principal stress vectors on the fracture surface

consistent with the morphology and orientation of the dimples in the fracture surface (Figs. 6 and 7).

## Conclusions

The microstructure and mechanical behavior of wire fixation slotted bolts which had previously failed in a clinical set were investigated. The bolts featured ductile fractures typical of components submitted to shear stress. According to the results obtained, the failure occurred through a combination of mechanical and microstructural factors, such as dimensional variations in the threaded area that concentrate stresses in the upper region of the screw, a high level of inclusions and poor surface finish. Although the raw material of the bolt adheres to the standard

specifications, the high level of sulfur allows inclusions to form, which weaken the material and works as stress concentrators, decreasing the resistance of the bolt.

In order to acquire a deeper insight into the strain and stress distribution in wire fixation bolts during loading, the load condition was reproduced virtually and analyzed using Finite Element Analysis. The numerical analysis demonstrated that the stress distribution is in agreement with the clinical failure of the screws. The dimple orientation and the direction of the principal stress on the fractured surface demonstrate the plastic collapse of the bolts with large shearing deformations. Thus, the failure torque of the screw should not be considered as an appropriate failure predictor and could be replaced by the maximum allowed angular displacement at the bolt head. However, further studies are needed to validate this failure predictor parameter.

**Acknowledgments** The authors would like to thank PRONEX-FAPESC, FINEP, and CNPq for financial support.

## References

1. M.M. Mullins, A.W. Davidson, D. Goodier, M. Barry, The biomechanics of wire fixation in the Ilizarov system. *Injury* **34**(2), 155–157 (2003)
2. J. Aronson, J.H. Harp, Mechanical considerations in using tensioned wires in a transosseous external fixation system. *Clin. Orthop. Relat. Res.* **280**, 23–29 (1992)
3. B. Fleming, D. Paley, T. Kristiansen, M. Pope, A biomechanical analysis of the Ilizarov external fixator. *Clin. Orthop. Relat. Res.* **241**, 95–105 (1989)
4. A.E. Goodship, J. Kenwright, The influence of induced micromovement upon the healing of experimental tibial fractures. *J. Bone Joint Surg. Br.* **67**, 650–655 (1985)
5. A.W. Davidson, M. Mullins, D. Goodier, M. Barry, Ilizarov wire tensioning and holding methods: a biomechanical study. *Injury* **34**, 151–154 (2003)
6. <http://www4.anvisa.gov.br/base/visadoc/REL/REL%5B11256-1-2%5D.PDF>. Accessed 01 April 2014
7. J. Gessmann, B. Jettkant, M. Königshausen, T.A. Schildhauer, D. Seybold, Improved wire stiffness with modified connection bolts in Ilizarov external frames: a biomechanical study. *Acta Bioeng. Biomech.* **14**(4), 15–21 (2012)
8. D.G. Bronson, M.L. Samchukov, R.B. Ashman, J.G. Birch, R.H. Browne, Stability of external circular fixation: a multi-variable biomechanical analysis. *Clin. Biomech.* **13**, 441–448 (1998)
9. M.A. Catagni, F. Guerreschi, L. Lovisetti, Distraction osteogenesis for bone repair in the 21st century: lessons learned. *Injury* **42**, 580–586 (2011)

10. N.A. Osei, B.M. Bradley, P. Culpan, J.B. Mitchell, M. Barry, K.E. Tanner, Relationship between locking-bolt torque and load pre-tension in the Ilizarov frame. *Injury* **37**(10), 941–945 (2006)
11. J.H. Calhoun, F. Li, B.R. Ledbetter, C.A. Gill, Biomechanics of the Ilizarov fixator for fracture fixation. *Clin. Orthop. Relat. Res.* **280**, 15–22 (1992)
12. P.J. Hillard, A.J. Harrison, R.M. Atkins, The yielding of tensioned fine wires in the Ilizarov frame. *Proc. Inst. Mech. Eng. H.* **212**, 37–47 (1998)
13. F.E. Donaldson, P. Pankaj, A.H.R.W. Simpson, Investigation of factors affecting loosening of Ilizarov ring–wire external fixator systems at the bone–wire interface. *J. Orthop. Res.* **30**(5), 726–732 (2012)
14. G.L. Orbay, V.H. Frankel, F.J. Kummer, The effect of wire configuration on the stability of the Ilizarov external fixator. *Clin. Orthop. Relat. Res.* **279**, 299–302 (1992)
15. G.F.V. Voort, E.P. Manilova, *Metallography and Microstructures of Stainless Steels and Maraging Steels, Metallography and Microstructures*, vol. 9 (ASM Handbook, Metal Park, 2004), pp. 670–700
16. T. Kosa, R.P. Ney, *Machining of Stainless Steels*, vol. 16, 9th edn. (ASM Handbook, Metal Park, 1989), pp. 681–707
17. E.M. Pohler, *Failures of Metallic Orthopedic Implantants, Failure Analysis and Prevention*, vol. 11 (ASM Handbook, Metal Park, 1986), pp. 2759–2767
18. ASTM F138-Standard Specification for Wrought 18Chromium–14Nickel–2.5Molybdenum Stainless Steel Bar and Wire for Surgical Implants, (2014)
19. J. Brnic, G. Turkalj, M. Canadija, D. Lanc, S. Krsanski, Responses of austenitic stainless steel American, Iron and Steel Institute (AISI) 303 (1.4305) subjected to different environmental conditions. *J. Test. Eval.* **40**(2), 256–264. <http://www.astm.org>
20. A.R. Rosenfield, *Fracture Mechanics in Failure Analysis, Fatigue and Fracture*, vol. 19 (ASM Handbook, Materials Park, 1996), pp. 1099–1108
21. K.H. Brown, C. Morrow, S. Durbin, A. Bac, Guideline for bolted joint design and analysis: version 1.0, a SAND2008-0371, (2008)
22. J.E. Shigley, *Mechanical Engineering Design (Portuguese Translation)*, 3rd edn. (McGraw-Hill Book, New York, 1984)